Similarity Solutions of Unsteady Three-Dimensional Stagnation Flow and Heat Transfer of a Viscous, Compressible Fluid on an Accelerated Flat Plate

H. R. Mozayyeni
Faculty of Engineering,
Ferdowsi University of Mashhad,
Mashhad 91775-1111, Iran

Asghar B. Rahimi[1]
Professor
Faculty of Engineering,
Ferdowsi University of Mashhad,
Mashhad 91775-1111, Iran
e-mails: rahimiab@yahoo.com;
rahimiab@um.ac.ir

The most general form of the problem of stagnation-point flow and heat transfer of a viscous, compressible fluid impinging on a flat plate is solved in this paper. The plate is moving with a constant or time-dependently variable velocity and acceleration toward the impinging flow or away from it. In this study, an external low Mach number flow impinges on the plate, along z-direction, with strain rate a and produces three-dimensional flow. The wall temperature is assumed to be maintained constant, which is different from that of the main stream. The density of the fluid is affected by the temperature difference existing between the plate and the incoming far-field flow. Suitably introduced similarity transformations are used to reduce the unsteady, three-dimensional, Navier–Stokes, and energy equations to a coupled system of nonlinear ordinary differential equations. The fourth-order Runge–Kutta method along with a shooting technique is applied to numerically solve the governing equations. The results are achieved over a wide range of parameters characterizing the problem. It is revealed that the significance of the aspect ratio of the velocity components in x and y directions, λ parameter, is much more noticeable for a plate moving away from impinging flow. Moreover, negligible heat transfer rate is reported between the plate and fluid viscous layer close to the plate when the plate moves away with a high velocity. [DOI: 10.1115/1.4032288]

Keywords: similarity solution, three-dimensional, stagnation-point flow, heat transfer, compressible fluid, accelerated plate

1 Introduction

The study of stagnation-point flow and heat transfer in the vicinity of a flat plate or a cylinder has been of a considerable interest in the last decades due to its technical importance over a wide range of industrial applications such as drying of papers and films, tempering of glass and metal during processing and high-pressure washers. The researches published related to this subject can be categorized into incompressible-based and compressible-based papers. The incompressible ones started by Hiemenz [1] and Homann [2] who discussed steady two-dimensional and axisymmetric three-dimensional, respectively, stagnation flow toward a circular cylinder. Howarth [3] was the first who considered a three-dimensional stagnation flow on a plate. In the more general context of a three-dimensional stagnation point, the flat plate can be allowed to slide in its own plane with constant velocity [4] and, also, can be assumed to be porous to allow for transpiration across it [5]. Axisymmetric stagnation flow toward a moving plate written by Wang [6] is one of the basic papers in this field. Fluid flow and mixed convection transport from a Plate in rolling and extrusion process have been studied by Karwe and Jaluria [7]. They have considered the heat transfer arising due to the movement of a continuous heated plate in processes such as hot rolling and hot extrusion. Kang et al. [8] have experimentally investigated the convective cooling of a heated continuously moving material. They considered the effects of thermal buoyancy, material speed and properties of the material and the fluid on the thermal field. Forced convection heat transfer from a continuously moving heated cylindrical rod in materials processing has been studied by Choudhury and Jaluria [9]. They presented numerical solutions for the vorticity, temperature, and stream function equations in the cylindrical coordinate system. Another numerical simulation of continuously moving flat sheet has been presented by Karwe and Jaluria [10]. Axisymmetric and nonaxisymmetric stagnation-point flow and heat transfer of a viscous, incompressible fluid on a moving cylinder in different physical situations is the main subject of the papers conducted by Saleh and Rahimi [11] and Rahimi and Saleh [12,13]. In another study, exact solutions of the Navier–Stokes and energy equations of a viscous obliquely impinging flow on a moving cylinder were studied by Rahimi and Esmaeilpour [14]. Exact solutions of the Navier–Stokes and energy equations were derived to solve the problem of stagnation-point flow and heat transfer of an incompressible fluid on a flat plate with and without transpiration by Shokrgozar Abbasi and Rahimi [15,16]. Also, Abbasi et al. [17] and Zhong and Fang [18] investigated the unsteady case of this problem.

Some papers available in the literature studied the compressible flow in the stagnation region of bodies using boundary layer equations. The characteristics of such a flow were scrutinized under different physical considerations in Refs. [19,20]. Kumari and Nath [21] studied the theory of the response of the compressible laminar boundary layer flow to the variation of the external stream velocity with time at a three-dimensional stagnation point, numerically. They solved such a problem when the flow is asymmetric with respect to the stagnation point in Ref. [22]. Subsequently, Kumari and Nath [23], in another paper, have gained the self-similar solution of the forgoing problem with mass transfer only when the free stream velocity varies inversely as a linear function of time. A similarity analysis of the steady,

[1]Corresponding author.

Contributed by the Heat Transfer Division of ASME for publication in the Journal of Heat Transfer. Manuscript received June 17, 2014; final manuscript received December 2, 2015; published online January 20, 2016. Assoc. Editor: Peter Vadasz.

three-dimensional, incompressible, laminar, boundary layer flow of time-independent non-Newtonian fluids was made by Timol and Kalthia [24] in rectangular co-ordinates. Two new implicit methods, namely, the implicit Godunov method and the implicit equilibrium flux method were used by Samtaney [25] in order to compute the self-similar solutions of the compressible Euler equations as a boundary value problem. Additionally, Zheng et al. [26] obtained similarity solutions to a second-order heat equation with convection in an infinite medium. They used suitable similarity transformations in order to reduce the parabolic heat equation to a class of singular nonlinear boundary value problems. These authors, in another research, solved the problem of compressible boundary layer behind a thin expansion wave by using the application of the similarity transformation and shooting technique in Ref. [27]. The objective of the paper presented by Hatori and Filho [28] was to analyze the laminar, compressible, axisymmetric, chemically reacting, boundary layer equations at the stagnation region of hypersonic flows by using the similarity concept. Furthermore, Turkyilmazoglu [29] was concerned with the case in which exact solution of the steady laminar flow of a compressible viscous fluid over a rotating disk was obtained in the presence of uniformly applied suction or blowing. The steady stagnation-point flow and heat transfer of a viscous, compressible fluid on an infinite stationary cylinder is the subject of the paper written by Mohammadiun and Rahimi [30]. In one of the most recent papers published in this field, Mozayyeni and Rahimi [31] accomplished to obtain the similarity parameters, for the first time, for the problem of unsteady two-dimensional stagnation flow and heat transfer of a compressible fluid on a moving flat plate. The potential flow impinging on the plate was assumed to be low Mach number one.

None of the studies mentioned above, deal with the case of unsteady, three-dimensional, stagnation-point flow and heat transfer of a viscous, compressible fluid on a flat plate. Hence, this paper is intended to solve such a problem, for the first time, where the plate can move toward or away from the impinging low Mach number flow at either constant or time-dependently variable velocity. In order to simulate these problems more accurately, it is mandatory to consider the density variations with respect to temperature. Hence, a Boussinesq approximation is taken into account to estimate the changes of density of the fluid, which is affected by the temperature difference existing between the plate and incoming far field flow. Suitably introduced similarity transformations are used in order to reduce the governing Navier–Stokes and energy equations to a coupled system of nonlinear ordinary differential equations, which are much easier to solve and an exact solution is sought. The results are presented for a wide range of parameters characterizing the problem. Our main motivation for performing this study is to use its results in modeling the fluid solidification of a three-dimensional stagnation-point flow on a flat plate in which the ice development and its thickening can be taken as if a plate is moving toward the flow. Incidentally, solving this problem using commercial software is more complicated and time consuming in addition to being less accurate. It is mainly because it requires much more grid meshes. For example, one-dimensional computational work related to reach results of our solution is around 100 meshes but using a commercial code to obtain approximate results would need around 10^6 meshes in three dimensions which introduce much more truncation errors into the problem. Above all, it is impossible to solve time-dependent boundary problems directly using a commercial code, for example FLUENT. Using similarity solution, the dimensionless quantities such as temperature, pressure, and velocity profiles are similar in all cross sections and as a result by obtaining only one profile of any quantity in a specific physical situation a perfect understanding of the distributions of these physical variables is able to be achieved in the entire physical domain. In addition, this problem depends on numerous physical independent variables and consequently it makes the analysis of the phenomenon complex if commercial fluids software is used. When using the similarity solution method, all the governing parameters and results are achieved in a dimensionless form and independent of the type of the fluid. Therefore, the number of independent variables is decreased which makes the analysis of the problem much simpler. General example for a three-dimensional stagnation flow and heat transfer, let us consider an impinging flow on a flat plate which is affected by a suction force in two opposite directions, Fig. 1. This suction force may be used to increase the heat transfer coefficient between the stagnation flow and the flat plate. This process can be observed in cooling towers which are repeatedly used in different sorts of cooling systems and power stations. If the physical limitations in both x and y directions are the same, then a three-dimensional axisymmetric case is encountered.

As we know, one of the most important applications of stagnation flows is the cooling processes of hot surfaces in many of which gases are used. For instance, the cooling process of a surface by air can be referred as a beneficial use of the stagnation flow which is applied by using a cold jet on a hot surface. In reality, the density of gases is affected by the temperature difference, which in such processes exists between the hot plate and the fluid source. In order to simulate these problems more accurately, it is necessary to take into account the variability of density with respect to temperature.

2 Problem Formulation

The problem of unsteady, three-dimensional, stagnation-point flow, and heat transfer of a viscous, compressible fluid on an accelerated flat plate is solved for the first time. The plate is moving toward the impinging low Mach number flow or away from it at either time-dependently variable or constant velocity. In order to solve this problem, the three-dimensional Cartesian coordinate system (x, y, z) with corresponding velocity components (u, v, w) is selected, as it is illustrated in Fig. 2 [34] and Fig. 3. [31]. An external potential flow impinges, along the z-direction, on the moving plate, firstly centered at $z = 0$, with strain rate a. Moreover, the temperature of the plate wall is maintained constant, which is different with that of the main stream, fixed at 25 °C.

After impingement of the compressible fluid on x–y plane, two regions are produced which are the potential region and the region of the viscous layer [32]. The potential region is an inviscid region where the velocity components in x and y directions do not change with respect to the z-axis, the axis normal to the plate, as it can be noticed in Fig. 3. Moreover, the viscous layer is a region close to the plate in which the velocity components change sharply to reach their values in the potential region. Figure 4 [34] represents the three-dimensional surface which is the boundary of these two different regions. An important note revealed in this figure is the difference existing between the values of x and y velocity components in the region of viscous layer. This phenomenon may happen if the flow pattern on the plate is bounded from both sides in one of the directions, for example x-axis, because of some physical limitations. An example of these physical limitations was

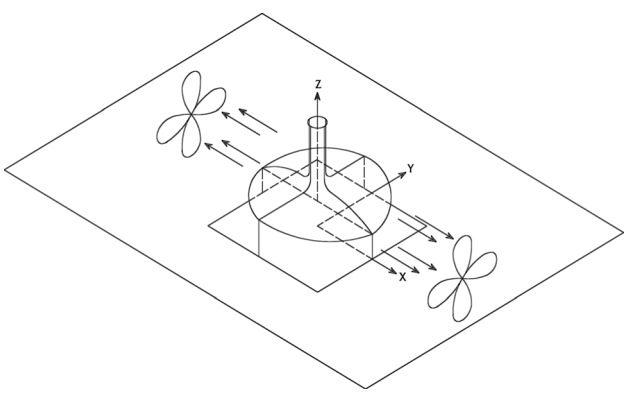

Fig. 1 Three-dimensional stagnation flow imposed by a suction force in two opposite directions

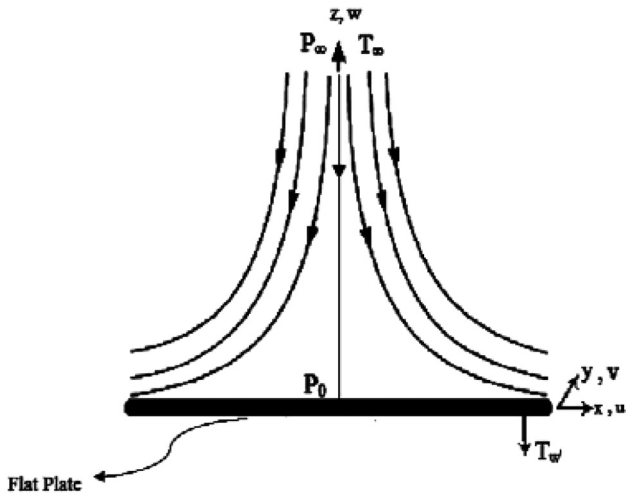

Fig. 2 Schematic of the problem

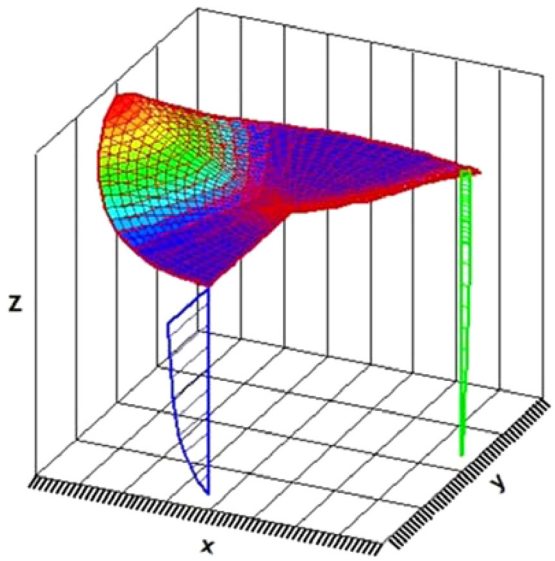

Fig. 4 Three-dimensional stream surface and velocity profiles

explained in Fig. 1. A parameter characterizing this situation is λ, the coefficient indicating the ratio of x to y velocity components in potential region and is defined between 0 and 1, $0 \leq \lambda \leq 1$, Ref. [3]. More explanations regarding this parameter will be given in Sec. 3. It is important to note that there is a difference between the concepts of a viscous layer and a boundary layer. In the Boundary Layer Theory, by making the boundary layer approximations, the governing Navier–Stokes equations of a viscous fluid flow are simplified. One of the important simplifying approximations of this theory is to eliminate the pressure variations in the direction normal to the surface inside the boundary layer. But in our work, the three-dimensional full Navier–Stokes and energy equations of a stagnation flow problem are solved by considering the pressure variations within the viscous layer close to the plate using the similarity solution method. One of the most significant characteristics of this research is to obtain the result without implementing the assumptions of the boundary layer theory. Hence, this problem should NOT be considered as a boundary layer flow. Moreover, there are some papers in the literature in which the stagnation flow over a flat plate was solved by the use of similarity solution when the plate moves in a normal direction such as Refs. [18,31,19].

The Navier–Stokes and energy equations governing this problem are as follows:

$$\frac{\partial \rho}{\partial t} + \frac{\partial (\rho u)}{\partial x} + \frac{\partial (\rho v)}{\partial y} + \frac{\partial (\rho w)}{\partial z} = 0 \tag{1}$$

$$\frac{\partial (\rho u)}{\partial t} + \frac{\partial (\rho uu)}{\partial x} + \frac{\partial (\rho vu)}{\partial y} + \frac{\partial (\rho wu)}{\partial z} = -\frac{\partial p}{\partial x} + \frac{\partial}{\partial x}\left(\mu \frac{\partial u}{\partial x}\right) + \frac{\partial}{\partial y}\left(\mu \frac{\partial u}{\partial y}\right) + \frac{\partial}{\partial z}\left(\mu \frac{\partial u}{\partial z}\right) \tag{2}$$

$$\frac{\partial (\rho v)}{\partial t} + \frac{\partial (\rho uv)}{\partial x} + \frac{\partial (\rho vv)}{\partial y} + \frac{\partial (\rho wv)}{\partial z} = -\frac{\partial p}{\partial y} + \frac{\partial}{\partial x}\left(\mu \frac{\partial v}{\partial x}\right) + \frac{\partial}{\partial y}\left(\mu \frac{\partial v}{\partial y}\right) + \frac{\partial}{\partial z}\left(\mu \frac{\partial v}{\partial z}\right) \tag{3}$$

$$\frac{\partial (\rho w)}{\partial t} + \frac{\partial (\rho uw)}{\partial x} + \frac{\partial (\rho vw)}{\partial y} + \frac{\partial (\rho ww)}{\partial z} = -\frac{\partial p}{\partial z} + \frac{\partial}{\partial x}\left(\mu \frac{\partial w}{\partial x}\right) + \frac{\partial}{\partial y}\left(\mu \frac{\partial w}{\partial y}\right) + \frac{\partial}{\partial z}\left(\mu \frac{\partial w}{\partial z}\right) \tag{4}$$

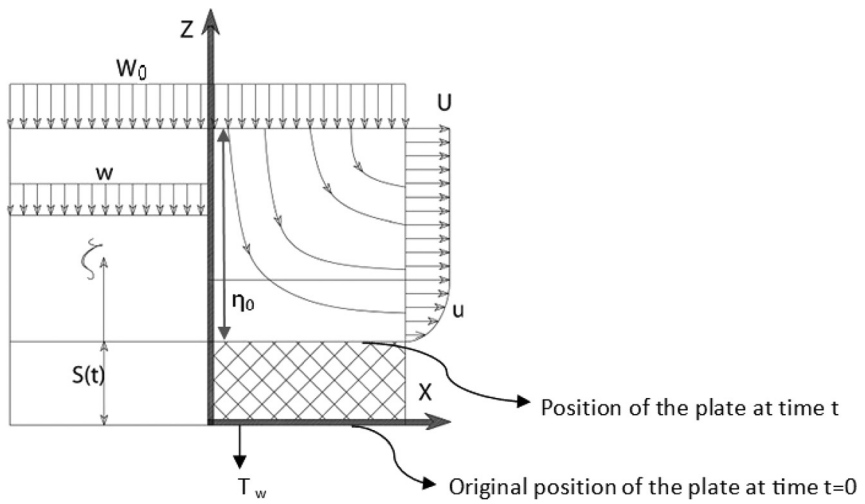

Fig. 3 Schematic of the problem

$$\rho c_p\left[\frac{\partial T}{\partial t}+u\frac{\partial T}{\partial x}+v\frac{\partial T}{\partial y}+w\frac{\partial T}{\partial z}\right]=\frac{\partial}{\partial x}\left(k\frac{\partial T}{\partial x}\right)+\frac{\partial}{\partial y}\left(k\frac{\partial T}{\partial y}\right)+\frac{\partial}{\partial z}\left(k\frac{\partial T}{\partial z}\right) \tag{5}$$

where p, ρ, μ, k, and T are pressure, density, dynamic viscosity, thermal conductivity, and temperature, respectively. It is worth noting that dynamic viscosity and thermal conductivity of the fluid are assumed to be constant. Furthermore, the dissipation terms of the energy equation are negligible at the stagnation region.

3 Similarity Solutions

The solution of the governing equations (1)–(4) in the potential region is expressed as

$$U=a(t)\lambda x \tag{6}$$

$$V=a(t)\,y \tag{7}$$

$$W=-a(t)(\lambda+1)\,\zeta \tag{8}$$

In which λ is a coefficient being the aspect ratio of the velocity components in x and y directions in the potential region $\lambda=(U/V)$ and is defined between 0 and 1. If gradients of the pressure are the same in all directions, the value of the potential velocities in different directions is equal as well. In this case, the flow will be axisymmetric and $\lambda=1$. Besides, if the variations of the flow in one direction, x-direction for example, are neglected, the flow will be considered as a two-dimensional case. In such a situation, there is no velocity component in x-direction. Therefore, the value of the parameter λ is 0. For all three-dimensional stagnation flows, the parameter λ is between 0 and 1, $0<\lambda<1$. With the increase of λ from 0 to 1, the problem crosses the line from two-dimensionality to axisymmetric three-dimensionality. Also, $\zeta=z-S(t)$ and $a(t)=(\partial w/\partial\zeta)$. Here, $S(t)$ is the amount of vertical displacement of the plate, positively defined when the plate moves toward the incoming far field flow along the z-direction and is a function of time. Hence, ζ and, then, flow strain rate $a(t)$ can be expressed as time-dependent functions.

A reduction of the Navier–Stokes and energy equations to ordinary differential equations is accomplished by using suitably introduced new similarity transformations as below:

$$\eta=\left(\rho_\infty\frac{a_o}{\mu}\right)^{\frac{1}{2}}\left(\int_0^z\left(\frac{\rho}{\rho_\infty}\right)dz-S(t)\right) \tag{9}$$

$$u=a\,(t)\lambda x f'(\eta,t) \tag{10}$$

$$v=a\,(t)y[f'(\eta,t)+g'(\eta,t)] \tag{11}$$

$$w=-\frac{1}{c}a(t)\left(\frac{\mu}{\rho_\infty a_0}\right)^{\frac{1}{2}}\big[\,(\lambda+1)f(\eta,t)+g(\eta,t)\big]+\dot{S}(t)\frac{\ln c}{c} \tag{12}$$

$$\theta=\frac{T(\eta,t)-T_\infty}{T_w-T_\infty} \tag{13}$$

where η is the similarity variable, the terms involving $f(\eta,t)$ and $g(\eta,t)$ comprise the Cartesian similarity form for the unsteady stagnation-point flow and prime denotes differentiation with respect to η, a_o is the reference potential flow strain rate at time $=0$, the subscripts w and ∞ refer to the conditions at the wall and in the free stream, respectively, $\dot{S}$ is the plate velocity and θ is the dimensionless temperature. It is to be noted that, according to Eq. (9), the similarity variable η is proportional to $z-S(t)$ which implies η is measured from the moving plate and not the plane $Z=0$, as depicted in Fig. 3. Equation (9) also implies that $\eta=0$ always coincides with the plate at any time during the movement of the plate.

In order to consider the effects of variations of temperature on the density of the fluid, a parameter $c(\eta)$ is introduced named as density ratio as

$$c(\eta)=\frac{\rho(\eta)}{\rho_\infty} \tag{14}$$

From Boussinesq approximation for low Mach number flow [33]

$$\rho\approx\rho_\infty\left[1-\beta(T-T_\infty)-\frac{\beta^2(T-T_\infty)^2}{2}-\frac{\beta^3(T-T_\infty)^3}{3!}-\ldots\right]$$

$$\Rightarrow\quad\frac{\rho}{\rho_\infty}=c(\eta)\approx1-\beta(T-T_\infty)-\frac{\beta^2(T-T_\infty)^2}{2}-\frac{\beta^3(T-T_\infty)^3}{3!}-\ldots \tag{15}$$

In which, β is the volumetric expansion coefficient. It is clear that for the case of an incompressible fluid, $\beta=0$. Hence, $\rho=\rho_\infty$ and $c(\eta)=1$. Also, it is interesting to note how the effect of the plate velocity $\dot{S}$ shows itself in w-component of velocity as in Eq. (12). In case of incompressible fluid, $c(\eta)=1$, this part has no role. Substituting the transformations (9)–(13) into the set of equations (1)–(5) causes the continuity equation to be satisfied, automatically, and gives a coupled system of ordinary differential equations reduced from x-momentum, y-momentum, and energy equations and, also, an expression for the pressure, obtained by integrating Eq. (4) in z-direction, as follows:

$$cf'''+\left(\tilde{a}\big[\,(\lambda+1)f+g\big]+\tilde{\dot{S}}(1-\ln c)+c'\right)f''+\left(-\frac{1}{\tilde{a}}\frac{\partial\tilde{a}}{\partial\tau}-\tilde{a}\lambda f'\right)f'+\frac{\lambda}{c}(\tilde{a})+\frac{1}{c}\left(1\tilde{a}\frac{\partial\tilde{a}}{\partial\tau}\right)=0 \tag{16}$$

$$cg'''+\left(\tilde{a}\big[\,(\lambda+1)f+g\big]+\tilde{\dot{S}}(1-\ln c)+c'\right)g''-\tilde{a}\big[2f'+g'\big]g'-\frac{1}{\tilde{a}}\frac{\partial\tilde{a}}{\partial\tau}g'+\tilde{a}(\lambda-1)\left((f')^2-\frac{1}{c}\right)=0 \tag{17}$$

$$c\theta''+c'\theta'+(\,\tilde{a}\,[(\lambda+1)f+g]+\tilde{\dot{S}}(1-\ln c))\,\mathrm{Pr}.\,\theta'=0 \tag{18}$$

$$\tilde{P}-\tilde{P}=0-\tilde{a}\tilde{\dot{S}}\left(\frac{(\lambda+1)f+g}{c}\right)+(\tilde{\dot{S}})^2\frac{\ln c}{c}-\frac{1}{2}\frac{\partial\tilde{a}}{\partial\tau}(\xi^2\lambda+\varsigma^2)-\frac{(\tilde{a})^2}{2}(\xi^2\lambda^2+\varsigma^2)$$
$$+\int_0^\eta\left(\begin{array}{l}\dfrac{\partial\tilde{a}}{\partial\tau}\dfrac{\big[\,(\lambda+1)f+g\big]}{c}-\tilde{\dot{S}}\dfrac{\ln c}{c}+\dfrac{\tilde{a}}{c^2}\big(\big[(\lambda+1)f'+g'\big]c-c'\big[\,(\lambda+1)f+g\big]\big)\\ \quad\cdot\left(\tilde{\dot{S}}\ln c-\tilde{a}\big[\,(\lambda+1)f+g\big]\right)+\dfrac{\tilde{\dot{S}}}{c^2}c'(1-\ln c).\left(\tilde{a}\big[\,(\lambda+1)f+g\big]-\tilde{\dot{S}}\ln c\right)\\ \quad+\dfrac{\tilde{\dot{S}}}{c}\left(c''(1-\ln c)-\dfrac{(c')^2}{c}(2-\ln c)\right)\\ \quad-\dfrac{\tilde{a}}{c}\left(\big[(\lambda+1)f''+g''\big]c-c''\big[\,(\lambda+1)f+g\big]-c'\big[(\lambda+1)f'+g'\big]+(c')^2\dfrac{\big[\,(\lambda+1)f+g\big]}{c}\right)\end{array}\right)d\eta \tag{19}$$

There are some dimensionless parameters introduced in the set of equations (16)–(19) which are defined below:

$$\tilde{a}(\tau)=\frac{a(t)}{a_0},\quad \tilde{P}=\frac{p}{\rho_\infty a_0 \upsilon},\quad \tilde{P}_0=\frac{p_0}{\rho_\infty a_0 \upsilon},\quad \tau=a_0 t,$$
$$\tilde{\dot{S}}=\frac{\dot{S}(t)}{\sqrt{a_0 \upsilon_\infty}},\quad \tilde{\ddot{S}}=\frac{\ddot{S}}{a_0\sqrt{\upsilon_\infty a_0}},\quad \xi=\sqrt{\frac{a_0}{\upsilon_\infty}}x,\quad \varsigma=\sqrt{\frac{a_0}{\upsilon_\infty}}y,$$
$$\frac{\partial \tilde{a}}{\partial \tau}=\frac{\tilde{\ddot{S}}}{\eta_0}+\frac{(\dot{S})^2}{\eta_0^2}+\frac{\tilde{\dot{S}}\tilde{W}_0}{\eta_0^2},\quad \mathrm{Pr}=\frac{\upsilon}{\alpha} \tag{20}$$

where $\tilde{a}(\tau), \tilde{P}, \tilde{P}_0, \tau, \tilde{\dot{S}}, \tilde{\ddot{S}}, \xi, \varsigma$, and Pr are dimensionless forms of the quantities strain rate, pressure, stagnation pressure, time, plate velocity, plate acceleration, x, y, and Prandtl number, respectively. In general, when the plate moves with time-dependently variable velocity, the strain rate a can be expressed as a function of time. Hence, $(\partial \tilde{a}/\partial \tau)$ represents the strain variation with respect to the time and is taken into account when the plate moves with time-dependent velocity and acceleration. The quantity η_0 used in this relation expresses the amount of vertical distance, from the plate, in which the velocity of the flow incoming to the plate is affected by the movement of the plate and starts decreasing. Also, $\tilde{W}_0$ is the dimensionless velocity of potential flow at η_o. It is worth noting that the system of equations (16)–(19) is the most general form for any arbitrary flat plate movement in vertical direction.

The boundary equations needed to solve the similarity equations are defined as follows:

$$\eta=0:\quad f=\frac{\tilde{\dot{S}}\ln c_w}{\tilde{a}(\lambda+1)},\quad f'=0,\quad g=0,\quad g'=0,\quad \theta=1 \tag{21}$$

$$\eta\to\infty:\quad f'=1,\quad g'=0,\quad \theta=0 \tag{22}$$

where

$$c_w=1-\beta(T_w-T_\infty)-\frac{\beta^2(T_w-T_\infty)^2}{2}-\frac{\beta^3(T_w-T_\infty)^3}{3!}-\ldots \tag{23}$$

4 Heat Transfer Coefficient

The local heat transfer coefficient on the flat plate is calculated from

$$h=\frac{q_w}{T_w-T_\infty} \tag{24}$$

Using dimensionless parameters, the dimensionless form of the heat transfer coefficient for this study can be gained as

$$H=-\theta'(\eta=0)c_w \tag{25}$$

in which

$$H=\frac{h}{k\left(\rho_\infty\dfrac{a}{\mu}\right)^{\frac{1}{2}}} \tag{26}$$

A finite difference procedure consisting of tridiagonal matrix algorithm is used to discretize the governing equations (16)–(19) describing the sets of laws. Moreover, the fourth-order Runge–Kutta method along with a shooting technique is applied to numerically solve the governing equations. To evaluate the mesh independency of the numerical scheme, the dimensionless heat transfer coefficient, Eq. (25), was initially tested for different mesh sizes of 15, 35, 55, 75, and 95 for $\beta=0.003, T_w=100\,^\circ\mathrm{C}, \mathrm{Pr}=0.7, \tilde{\dot{S}}=0.0, \lambda=1$. It is readily found out that, as the results indicate in Table 1, the most efficient grid size is 75 where there is not much difference between the amounts of the dimensionless heat transfer coefficient when the number of meshes increases from 75 to 95. It is worth noting that in order to achieve better results, the grids are generated denser in the region close to the plate. The numerical procedure is repeated until the difference between the results of two repeated sequences of each of the equations becomes less than 0.0001.

Table 1 Grid independence results

No. of grids	15	35	55	*75*	95
Dimensionless heat transfer coefficient (H)	0.74621	0.69841	0.66134	0.64571	0.64492

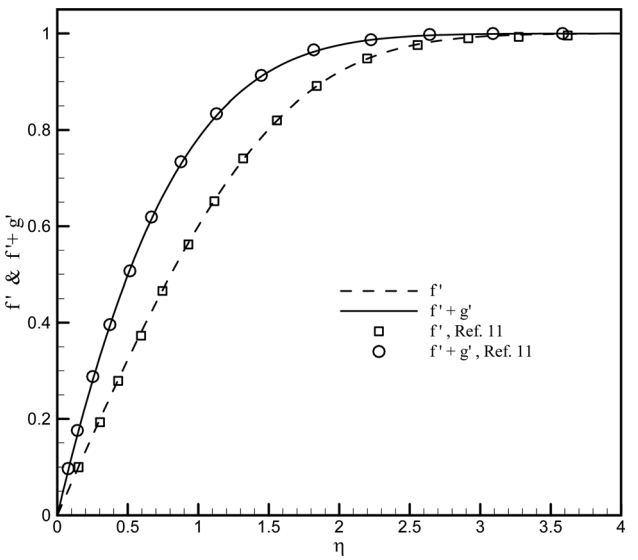

Fig. 5 Comparison of f' and $f'+g'$ profiles between the present work and Ref. [11] for $\lambda=0.1$

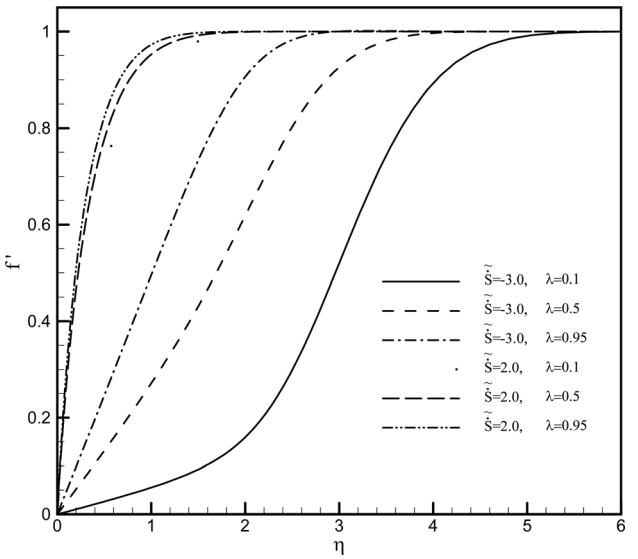

Fig. 6 f' distributions for different values of plate velocity and λ parameter when $\beta=0.003$, $T_w=125\,^\circ\mathrm{C}$, $\mathrm{Pr}=0.7$

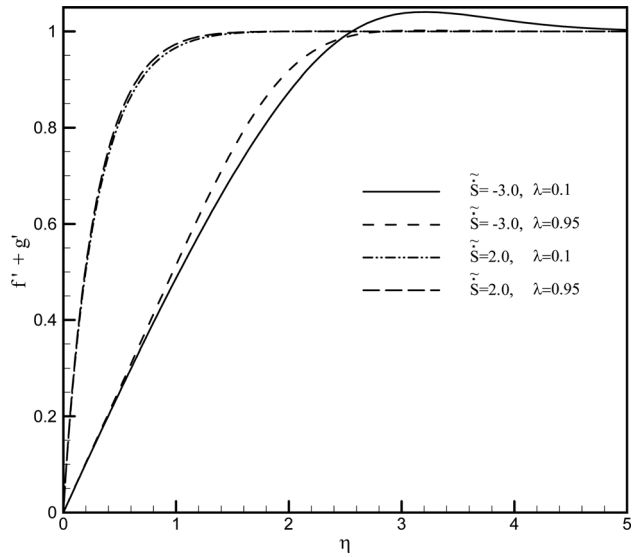

Fig. 7 $f' + g'$ **distributions for different values of plate velocity and** λ **parameter when** $\beta = 0.003$, $T_w = 125\,^{\circ}\mathrm{C}$, $\mathrm{Pr} = 0.7$

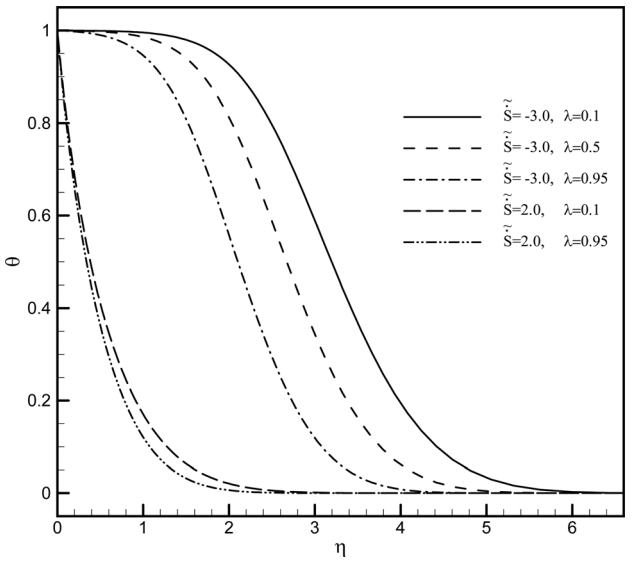

Fig. 9 θ **distributions for different values of plate velocity and** λ **parameter when** $\beta = 0.003$, $T_w = 125\,^{\circ}\mathrm{C}$, $\mathrm{Pr} = 0.7$

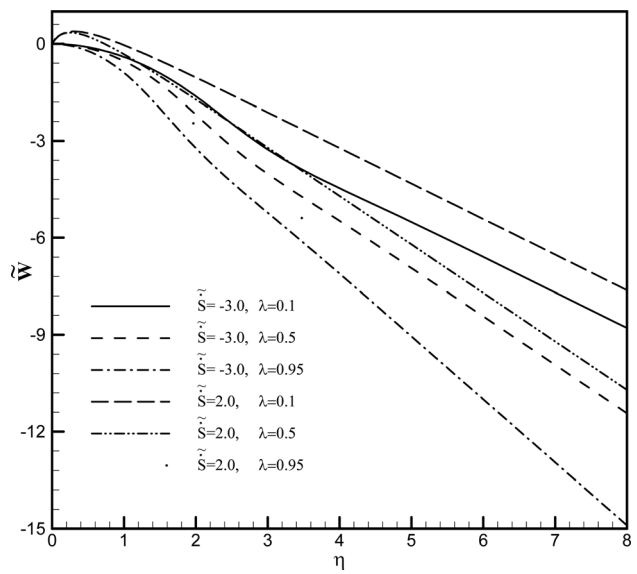

Fig. 8 Distributions of dimensionless w component of velocity for different values of plate velocity and λ **parameter when** $\beta = 0.003$, $T_w = 125\,^{\circ}\mathrm{C}$, $\mathrm{Pr} = 0.7$

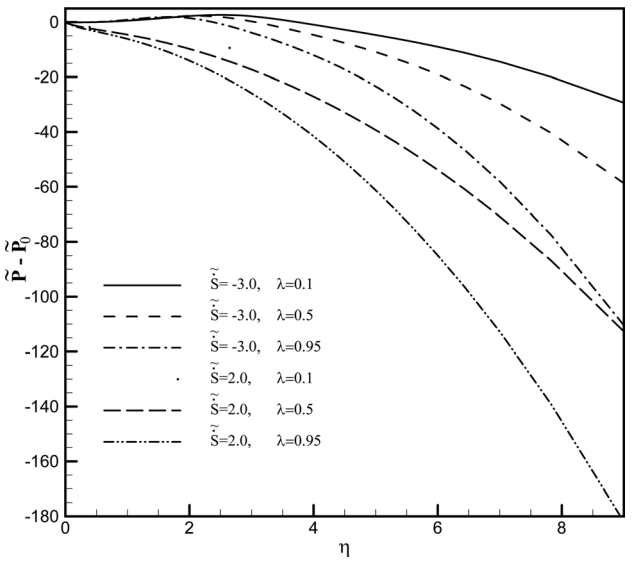

Fig. 10 Dimensionless pressure distributions for different values of plate velocity and λ **parameter when** $\beta = 0.003$, $T_w = 125\,^{\circ}\mathrm{C}$, $\mathrm{Pr} = 0.7$

5 Presentation of Results

In this section, the results are presented for different physical phenomena including moving plate with constant and time-dependently variable velocity.

First, the simplified case of this problem, the incompressible fluid impinging on a stationary plate, is compared to that of Ref. [11] in Fig. 5 to validate the numerical procedure. Here, the λ parameter is 0.1.

In Figs. 6–8, distributions of different velocity components are depicted for selected values of λ number when the plate is moving toward the impinging flow, $\tilde{\dot{S}} = 2$, or away from it, $\tilde{\dot{S}} = -3$. As it can be seen from Figs. 6 and 7, for a plate moving away from the main stream, the increase of λ number causes the considerable decrease in f' boundary layer thickness; however, not much changes are reported for that of the y-direction velocity component. Besides, for a plate moving with a positive-valued velocity, if the flow departs from the case of three-dimensional, $\lambda = 0.1$, to the axisymmetric one, not much noticeable changes are captured for distributions of x and y velocity components. If dimensionless form of w-component is introduced as $\tilde{W} = w/\sqrt{a_0 \upsilon_\infty}$, $\tilde{W}$ distributions are depicted in Fig. 7 for selected values of the plate velocity and λ parameter. In this figure, with the increase of λ number from 0.1 to 0.95, the absolute value of w component increases whether the plate moves toward or away from the potential flow.

In order to investigate the influences of λ and $\tilde{\dot{S}}$ numbers on the temperature and pressure, dimensionless forms of these two quantities are illustrated in Figs. 9 and 10. In Fig. 9, for the case of $\tilde{\dot{S}} = -3$, the more the velocity ratio, the less the thermal boundary layer thickness will be. However, the increase of λ parameter from 0.1 to 0.95 does not have any noticeable effect on the temperature distributions when $\tilde{\dot{S}} = 2$. The obtained results also revealed that for a plate moving away from the impinging flow, especially with high values of $\tilde{\dot{S}}$, the θ' tends to zero in the region close to the plate.

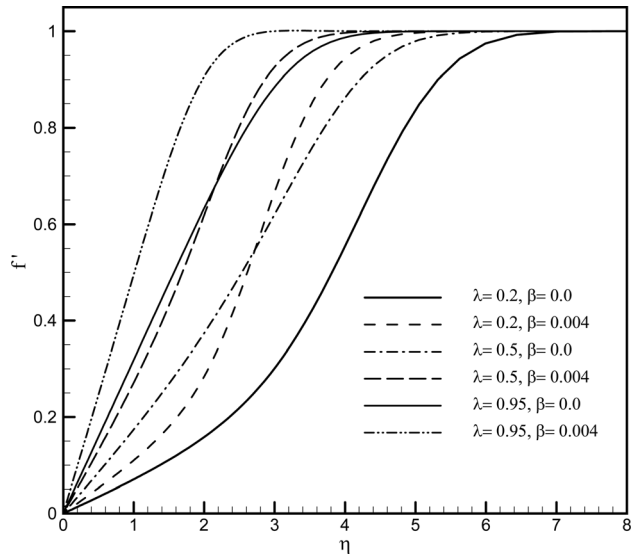

Fig. 11 f' distributions for the case of $\tilde{\dot{S}} = -3$ for different values of λ and β parameters when $T_w = 100\,^{\circ}\mathrm{C}$, Pr = 0.7

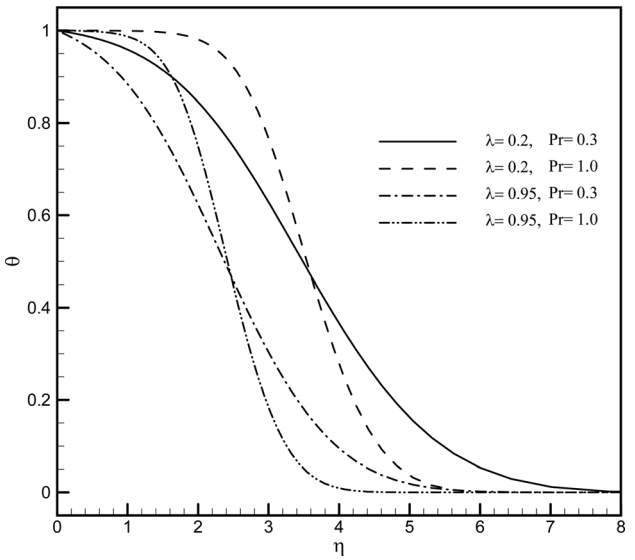

Fig. 13 θ distributions for the case of $\tilde{\dot{S}} = -3$ for different values of λ and Pr numbers when $\beta = 0.003$, $T_w = 100\,^{\circ}\mathrm{C}$

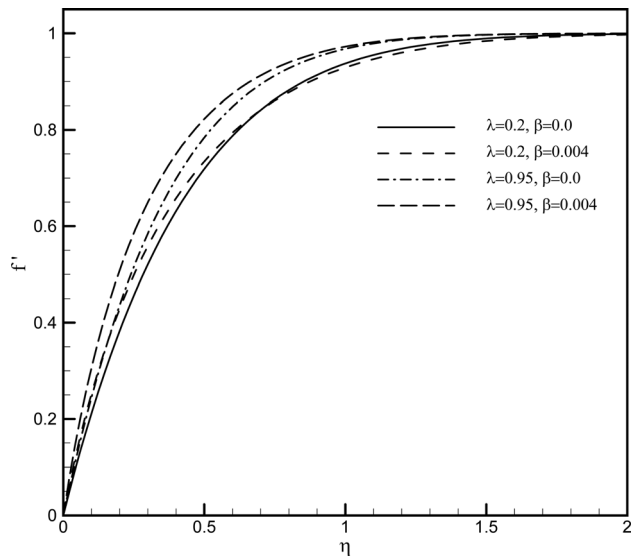

Fig. 12 f' distributions for the case of $\tilde{\dot{S}} = 2$ for different values of λ and β parameters when $T_w = 100\,^{\circ}\mathrm{C}$, Pr = 0.7

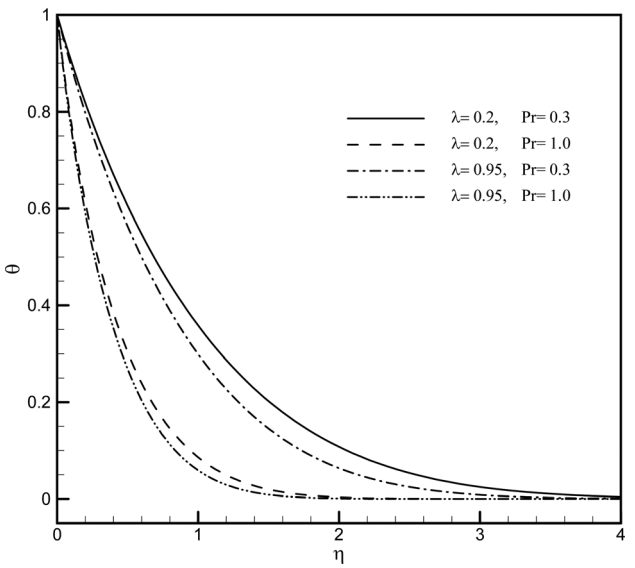

Fig. 14 θ distributions for the case of $\tilde{\dot{S}} = 2$ for different values of λ and Pr numbers when $\beta = 0.003$, $T_w = 100\,^{\circ}\mathrm{C}$

This means that there is not a noticeable heat transfer rate between the plate and viscous fluid close to the plate in such situations. Another interesting point discovered from these two figures is that the thermal boundary layer thickness depends strongly on the direction of the plate movement and increases considerably when the plate moves away from the impinging flow. For a plate moving with a negative-valued velocity, the pressure distributions in the region close to the plate do not change significantly if the velocity ratio increases. In the distances being far away from the plate, the enhancement of the λ number causes the absolute value of dimensionless pressure to increase. This behavior can be similarly seen when the plate is moving toward the impinging flow.

The effects of λ and β parameters on f' profiles are investigated in Fig. 9, when $\tilde{\dot{S}} = -3$, and Fig. 10, when $\tilde{\dot{S}} = 2$, for $T_w = 100\,^{\circ}\mathrm{C}$ and Pr = 0.7. As it is shown in Fig. 11, the increase of β number from 0.0, the incompressible-stated fluid, to 0.004 has the same effect on f' distributions for different values of λ parameter and causes the increase in the amount of f' at any value of η. According to Fig. 12, if the β number varies in a range of 0.0–0.004, for any specified value of velocity ratio, the f' profile does not undergo any considerable changes.

The temperature distributions for selected values of $\tilde{\dot{S}}$, Pr, and λ numbers are the subject of Figs. 13 and 14 when $\beta = 0.003$, and $T_w = 100\,^{\circ}\mathrm{C}$. As it can be noticed from these two figures, if the Pr number of a fluid increases, for a fix-valued velocity ratio, the thermal boundary layer thickness decreases whether the plate moves toward the main potential flow or away from it.

It can also be shown that with the increase of β number, a different behavior is revealed for pressure distributions depending on the moving direction of the plate. For a plate moving away from the impinging flow, the absolute value of the pressure for a fluid with $\beta = 0.004$ is higher in comparison with that of an incompressible fluid. However, when $\tilde{\dot{S}} = 2$, the increase of β from 0.0 to 0.004 causes the absolute value of the pressure to decrease. Note that for a plate moving with a negative velocity, the changes in β and λ numbers do not affect the pressure values in the region being close to the plate and the pressure in this region is, somehow, equal to stagnation pressure.

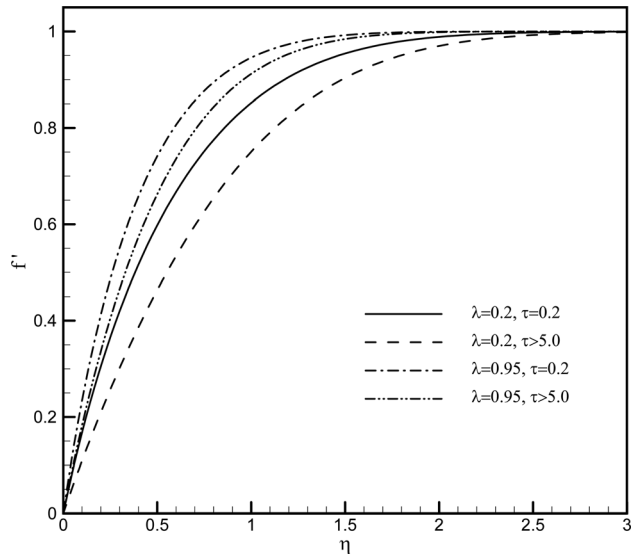

Fig. 15 Effects of λ parameter on unsteady f' profiles when $\beta = 0.003$, $T_w = 125\,^{\circ}\mathrm{C}$, $\mathrm{Pr} = 0.7$

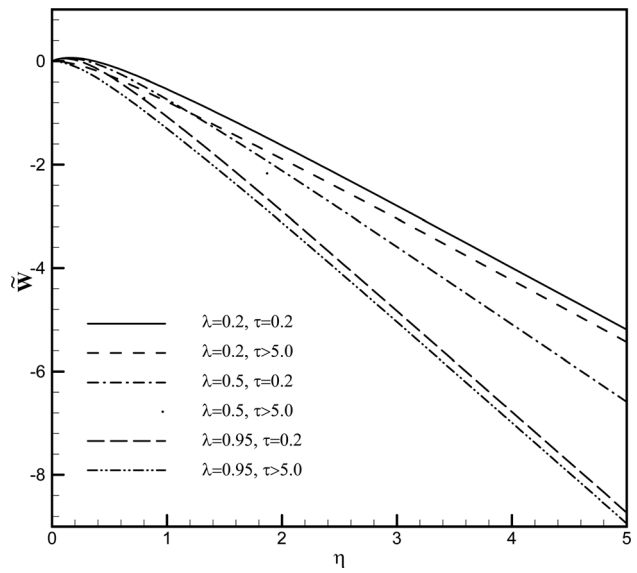

Fig. 16 Effects of λ parameter on dimensionless form of unsteady w component when $\beta = 0.003$, $T_w = 125\,^{\circ}\mathrm{C}$, $\mathrm{Pr} = 0.7$

In unsteady cases, the plate can move with any arbitrary time-dependent velocity function. As a most practical example for time-dependently moving plate, the exponential function, which can be used to model a three-dimensional solidification problem, is selected in the form given below:

$$\dot{S} = \exp(-t) \tag{27}$$

The results obtained by using the plate velocity function mentioned above are presented in Figs. 15–18. Figures 15 and 16 illustrate the distributions of velocity components at different times for selected values of velocity ratio when $\beta = 0.003$, $T_w = 125\,^{\circ}\mathrm{C}, \mathrm{Pr} = 0.7$. With the passage of time, the velocity and acceleration of the plate tend to zero and, so, the steady-state conditions govern on the flow patterns. Hence, for $\tau > 5.0$ and for a fix-valued λ number, the velocity components in x and y directions have lower values in comparison with those at the beginning of the motion. In contrast, Fig. 16 shows a slightly increase in the absolute amounts of dimensionless w-component

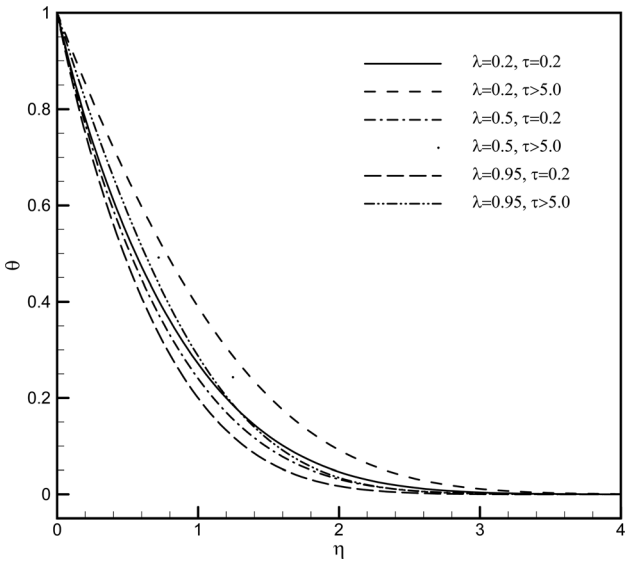

Fig. 17 Effects of λ parameter on unsteady θ profiles when $\beta = 0.003$, $T_w = 125\,^{\circ}\mathrm{C}$, $\mathrm{Pr} = 0.7$

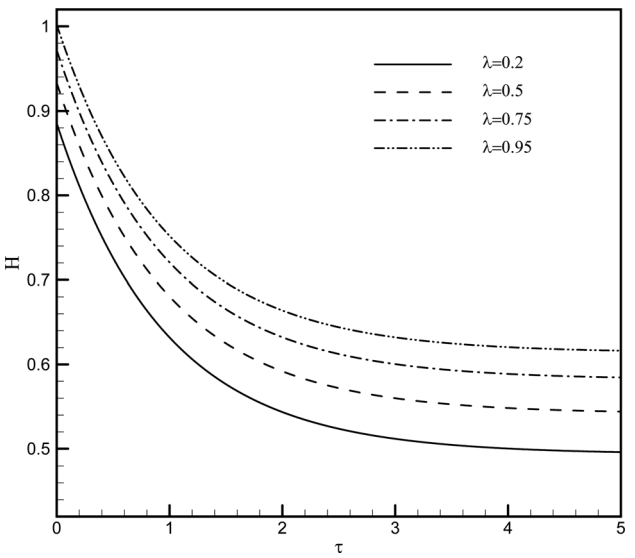

Fig. 18 Distributions of dimensionless heat transfer coefficient in unsteady procedure for different values of λ parameter when $\beta = 0.003$, $T_w = 125\,^{\circ}\mathrm{C}$, $\mathrm{Pr} = 0.7$

at steady-state conditions, $\tau > 5.0$, by comparison with those at $\tau = 0.2$.

Distribution of the dimensionless temperature is presented in Fig. 17 for different values of λ parameter and time. As the time increases for a particular value of λ, the flow and heat transfer become close to steady-state conditions, gradually. This phenomenon causes the temperature quantity to increase and the absolute value of the pressure to decrease, at any specified value of η.

Distributions of the dimensionless heat transfer coefficient H versus time in terms of a wide range of the velocity ratio is presented in Fig. 18 when $\beta = 0.003, T_w = 125\,^{\circ}\mathrm{C}, \mathrm{Pr} = 0.7$. As it can be seen, when the plate is at the beginning of its exponentially time-dependent moving, there is a considerable amount of heat transfer between the plate and the viscous layer of the fluid close to the plate. With the passing of time, when the plate velocity and acceleration tend to zero, the H coefficient decreases until it reaches a stable value. Note that the more the velocity ratio, the less the coefficient H will be.

6 Conclusions

An exact solution of the unsteady, three-dimensional, Navier–Stokes, and energy equations has been achieved for the problem of stagnation-point flow and heat transfer of a viscous, compressible fluid impinging on an accelerated flat plate. This was accomplished by using appropriately introduced similarity transformations. The density of the fluid was assumed to change with respect to the temperature difference existing between the plate and the fluid source. A Boussinesq approximation was applied to capture the density variations. The results were presented for a wide range of parameters characterizing the problem including λ parameter, thermal expansion coefficient (β), wall temperature, Prandtl number, and plate velocity. It was revealed that the cooling process of a hot plate is much faster when the plate moves toward the cold impinging flow. In fact, the heat transfer rate between the plate and the viscous fluid close to the plate tends to vanish if the plate moves with a high negative velocity. In other words, the cooling process of a hot plate which moves away with a high velocity from the impinging flow is very slow. Moreover, it was shown that the shear–stress on a plate which moves upward is much more considerable compared to a plate moving downward. Furthermore, the velocity and thermal boundary layer thicknesses strongly depend on the value of the λ parameter when the plate moves downward.

Nomenclature

$a(t)$ = time-dependent flow strain rate
a_o = flow strain rate at time = 0
c = density ratio
f, g = similarity functions
h = local heat transfer coefficient
H = dimensionless heat transfer coefficient
k = thermal conductivity of the fluid
p = pressure
$\tilde{P}$ = dimensionless pressure
Pr = Prandtl number
$S, \dot{S}, \ddot{S}$ = displacement, velocity, and acceleration of the plate, respectively, in z-direction
$\tilde{S}, \tilde{\dot{S}}, \tilde{\ddot{S}}$ = dimensionless forms of displacement, velocity, and acceleration of the plate, respectively, in z-direction
T = temperature
u, v, w = velocity components near the plate in x, y, z directions
U, V, W = velocity components in potential region in x, y, z directions
x, y, z = Cartesian coordinates

Greek Symbols

β = volumetric expansion coefficient
ζ = variable $(z - S(t))$
η = similarity variable
θ = dimensionless temperature
λ = velocity ratio
μ = dynamic viscosity
υ = kinematic viscosity
ξ = dimensionless x-axis
ς = dimensionless y-axis
ρ = density
τ = dimensionless time

Subscripts

w = wall
∞ = infinite
0 = stagnation point

References

[1] Hiemenz, K., 1911, "Boundary Layer for a Homogeneous Flow Around a Dropping Cylinder," Dinglers Polytech. J., **326**, pp. 321–410.
[2] Homann, F. Z., 1936, "Effect of High Speed Over Cylinder and Sphere," Z. Angew. Math. Mech., **16**(3), pp. 153–164.
[3] Howarth, L., 1951, "The Boundary Layer in Three-Dimensional Flow. Part II: The Flow Near a Stagnation Point," Philos. Mag., **42**(7), pp. 1433–1440.
[4] Libby, P. A., 1974, "Wall Shear at a Three-Dimensional Stagnation Point With a Moving Wall," AIAA J., **12**(3), pp. 408–409.
[5] Libby, P. A., 1976, "Laminar Flow at a Three-Dimensional Stagnation Point With Large Rates of Injection," AIAA J., **14**(9), pp. 1273–1279.
[6] Wang, C. Y., 1973, "Axisymmetric Stagnation Flow Towards a Moving Plate," AIChE J., **19**(5), pp. 1080–1081.
[7] Karwe, M. V., and Jaluria, Y., 1988, "Fluid Flow and Mixed Convection Transport From a Plate in Rolling and Extrusion Process," ASME J. Heat Transfer, **110**(3), pp. 655–661.
[8] Kang, B. H., Yoo, J., and Jaluria, Y., 1994, "Experimental Study of the Convective Cooling of a Heated Continuously Moving Material," ASME J. Heat Transfer, **116**(1), pp. 199–208.
[9] Choudhury, S. R., and Jaluria, Y., 1994, "Forced Convection Heat Transfer From a Continuously Moving Heated Cylindrical Rod in Materials Processing," ASME J. Heat Transfer, **116**(3), pp. 724–734.
[10] Karwe, M. V., and Jaluria, Y., 1991, "Numerical Simulation of Thermal Transport Associated With a Continuously Moving Flat Sheet in Material Processing," ASME J. Heat Transfer, **113**(3), pp. 612–619.
[11] Saleh, R., and Rahimi, A. B., 2004, "Axisymmetric Stagnation-Point Flow and Heat Transfer of a Viscous Fluid on a Moving Cylinder With Time-Dependent Axial Velocity and Uniform Transpiration," ASME J. Fluids Eng., **126**(6), pp. 997–1005.
[12] Rahimi, A. B., and Saleh, R., 2007, "Axisymmetric Stagnation-Point Flow and Heat Transfer of a Viscous Fluid on a Rotating Cylinder With Time-Dependent Angular Velocity and Uniform Transpiration," ASME J. Fluids Eng., **129**(1), pp. 106–115.
[13] Rahimi, A. B., and Saleh, R., 2008, "Similarity Solution of Unaxisymmetric Heat Transfer in Stagnation-Point Flow on a Cylinder With Simultaneous Axial and Rotational Movements," ASME J. Heat Transfer, **130**(5), p. 054502.
[14] Rahimi, A. B., and Esmaeilpour, M., 2011, "Axisymmetric Stagnation Flow Obliquely Impinging on a Moving Circular Cylinder With Uniform Transpiration," Int. J. Numer. Methods Fluids, **65**(9), pp. 1084–1095.
[15] Abbasi, A. S., and Rahimi, A. B., 2009, "Non-Axisymmetric Three-Dimensional Stagnation-Point Flow and Heat Transfer on a Flat Plate," ASME J. Fluids Eng., **131**(7), p. 074501.
[16] Abbasi, A. S., and Rahimi, A. B., 2009, "Three-Dimensional Stagnation Flow and Heat Transfer on a Flat Plate With Transpiration," J. Thermophys. Heat Transfer, **23**(3), pp. 513–521.
[17] Abbasi, A. S., Rahimi, A. B., and Niazmand, H., 2011, "Exact Solution of Three-Dimensional Unsteady Stagnation Flow on a Heated Plate," J. Thermodyn. Heat Transfer, **25**(1), pp. 55–58.
[18] Zhong, Y., and Fang, T., 2011, "Unsteady Stagnation-Point Flow Over a Plate Moving Along the Direction of Flow Impingement," Int. J. Heat Mass Transfer, **54**, pp. 3103–3108.
[19] Libby, P. A., 1967, "Heat and Mass Transfer at a General Three-Dimensional Stagnation Point," AIAA J., **5**(3), pp. 507–517.
[20] Nath, G., 1971, "Compressible Axially Symmetric Laminar Boundary Layer Flow in the Stagnation Region of a Blunt Body in the Presence of Magnetic Field," Acta Mech., **12**, pp. 267–273.
[21] Kumari, M., and Nath, G., 1978, "Unsteady Laminar Compressible Boundary-Layer Flow at a Three-Dimensional Stagnation Point," J. Fluid Mech., **87**(04), pp. 705–717.
[22] Kumari, M., and Nath, G., 1980, "Unsteady Compressible 3-Dimensional Boundary-Layer Flow Near an Asymmetric Stagnation Point With Mass transfer," Int. J. Eng. Sci., **18**(11), pp. 1285–1300.
[23] Kumari, M., and Nath, G., 1981, "Self-Similar Solution of Unsteady Compressible Three-Dimensional Stagnation-Point Boundary Layers," J. Appl. Math. Phys. **32**(3), pp. 267–276.
[24] Timol, M. G., and Kalthia, N. L., 1986, "Similarity Solutions of Three-Dimensional Boundary Layer Equations of Non-Newtonian Fluids," Int. J. Nonlinear Mech., **21**(6), pp. 475–481.
[25] Samtaney, R., 1997, "Computational Methods for Self-Similar Solutions of the Compressible Euler Equations," J. Comput. Phys., **132**(2), pp. 327–345.
[26] Zheng, L., Zhang, X., and He, J., 2003, "Similarity Solution to a Heat Equation With Convection in an Infinite Medium," J. Univ. Sci. Technol. Beijing, **10**(4), pp. 29–32.
[27] Zheng, L., Zhang, X., and He, J., 2004, "Analytical Solutions to a Compressible Boundary Layer Problem With Heat Transfer," J. Univ. Sci. Technol. Beijing, **11**(2), pp. 120–122.
[28] Hatori, M. E., and Pessoa-Filho, J. B., 2005, "Similarity Solutions for the Chemically Reacting Compressible Boundary Layer Equations," AIAA Paper No. 2005-580.
[29] Turkyilmazoglu, M., 2009, "Purely Analytic Solutions of the Compressible Boundary Layer Flow Due to a Porous Rotating Disk With Heat Transfer," J. Phys. Fluids, **21**(10), p. 106104.
[30] Mohammadiun, H., and Rahimi, A. B., 2012, "Axisymmetric Stagnation-Point Flow and Heat Transfer of a Viscous, Compressible Fluid on a Cylinder With Constant Wall Temperature," J. Thermophys. Heat Transfer, **26**(3), pp. 494–502.
[31] Mozayyeni, H. R., and Rahimi, A. B., 2014, "Unsteady Two-Dimensional Stagnation-Point Flow and Heat Transfer of a Viscous, Compressible Fluid on an Accelerated Flat Plate," ASME J. Heat Transfer, **136**(4), p. 041701.
[32] Schlichting, H., 1979, *Boundary Layer Theory*, 7th ed., McGraw-Hill, New York.
[33] Jaluria, Y., 1980, *Natural Convection Heat and Mass Transfer*, Pergamon Press, Oxford, UK.
[34] Mozayyeni, M. R., and Rahimi, A. B., 2013, "Three-Dimensional Stagnation Flow and Heat Transfer of a Viscous, Compressible Fluid on a Flat Plate," ASME J. Heat Transfer, **135**(10), p. 101702.